On illumination schemes for wide-field CARS microscopy

I. Toytman,[1,*] D. Simanovskii,[1] and D. Palanker[1,2]

[1] *Hansen Experimental Physics Laboratory, Stanford University, CA 94305-4085, USA*
[2] *Department of Ophthalmology, Stanford University School of Medicine, Stanford, CA 94305, USA*
[*] *Corresponding author: itoytman@stanford.edu*

Abstract: New system for a wide-field CARS microscopy is demonstrated, including two schemes of non-phase-matching illumination. Several advantages including high Stokes pulse energy, pulse-to-pulse stability and inherent synchronization between pump and Stokes pulses were brought by use of methane-filled Raman converter. Spatial resolution of the system with axially symmetric illumination, 0.5μm, was found to correspond to diffraction limit of the imaging objective. Selective sensitivity to lipid-rich myelin sheaths in the nerve tissue has been demonstrated and confirmed by comparison with histological samples stained with myelin-specific dye. Single-shot imaging capability of the system has been demonstrated with a speckling-free illumination on a monolayer of 3μm polystyrene beads.

OCIS codes: (180.0180) Microscopy; (190.5650) Raman effect; (190.5890) Scattering, stimulated.

References and links

1. E. Kohen and J. G. Hirschberg, *Cell Structure and Function by Microspectrofluorometry* (Academic, San Diego, Calif., 1989).
2. W. C. W. Chan and S. Nie, "Quantum Dot Bioconjugates for Ultrasensitive Nonisotopic Detection," Science **281**, 2016-2018 (1998).
3. D. Dosev, M. Nichkova, M. Liu, B. Guo, G. Liu, Y. Xia, B. D. Hammock, and I. M. Kennedy, "Application of fluorescent Eu:Gd_2O_3 nanoparticles to the visualization of protein micropatterns," Proc. SPIE **5699**, 473-481 (2005).
4. D. Huang, E. A. Swanson, C. P. Lin, J. S. Schuman, W. G. Stinson, W. Chang, M. R. Hee, T. Flotte, K. Gregory, C. A. Puliafito, and J. G. Fujimoto, "Optical Coherence Tomography," Science **254**, 1178-1181 (1991).
5. J.-X. Cheng, Y. K. Jia, G. Zheng, and X. S. Xie, "Laser-Scanning Coherent Anti-Stokes Raman Scattering Microscopy and Applications to Cell Biology," Biophys. J. **83**, 502-509 (2002).
6. E. O. Potma and X. S. Xie, "Detection of single lipid bilayers with coherent anti-Stokes Raman scattering (CARS) microscopy," J. Raman Spectrosc. **34**, 642-650 (2003).
7. C. P. Pfeffer, B. R. Olsen, F. Ganikhanov, and F. Legare, "Multimodal nonlinear optical imaging of collagen arrays," J. Struct. Biol. **164**, 140-145 (2008).
8. E. O. Potma, X. S. Xie, L. Muntean, J. Preusser, D. Jones, J. Ye, S. R. Leone, W. D. Hinsberg, and W. Schade, "Chemical Imaging of Photoresists with Coherent Anti-Stokes Raman Scattering (CARS) Microscopy," J. Phys. Chem. B **108**, 1296-1301 (2004).
9. C. Heinrich, S. Bernet, and M. Ritsch-Marte, "Wide-field coherent anti-Stokes Raman scattering microscopy," Appl. Phys. Lett. **84**, 816-818 (2004).
10. C. Heinrich, A. Hofer, A. Ritsch, C. Ciardi, S. Bernet, and M. Ritsch-Marte, "Selective imaging of saturated and unsaturated lipids by wide-field CARS-microscopy," Opt. Express **16**, 2699-2708 (2008).
11. I. Toytman, K. Cohn, T. Smith, D. Simanovskii, and D. Palanker, "Wide-field coherent anti-Stokes Raman scattering microscopy with non-phase-matching illumination," Opt. Lett. **32**, 1941-1943 (2007).
12. C. L. Evans and X. S. Xie, "Coherent Anti-Stokes Raman Scattering Microscopy: Chemically Selective Imaging for Biology and Medicine," Annu. Rev. Anal. Chem. **1**, 883-909 (2008).
13. C. L. Evans, E. O. Potma, M. Puoris'haag, D. Cote, C. P. Lin, and X. S. Xie, "Chemical imaging of tissue in vivo with video-rate coherent anti-Stokes Raman scattering microscopy," Proc. Nat. Acad. Sci. **102**, 16807-16812 (2005).
14. H. Wang, Y. Fu, P. Zickmund, R. Shi, and J.-X. Cheng, "Coherent Anti-Stokes Raman Scattering Imaging of Axonal Myelin in Live Spinal Tissue," Biophys. J. **89**, 581-591 (2005).

#106549 - $15.00 USD Received 21 Jan 2009; revised 5 Mar 2009; accepted 7 Apr 2009; published 20 Apr 2009

1. Introduction

Contrast mechanisms currently utilized in optical microscopy can be grouped into two general categories: exogenous staining associated with specific markers, and intrinsic optical properties of the tissue. Both approaches have a wide range of applications, and continue to progress in many fields of biological and medical research. Fluorescent and absorbing dyes, nanoparticles, and quantum dots attached to specific affinity markers are broadly used in-vitro and in-vivo [1-3]. Traditional single photon excitation methods are being supplemented by multiphoton techniques, allowing for better spatial resolution, reduced bleaching, and three-dimensional sectioning capability. However, exogenous staining often alters normal metabolism of the living cells, which limits its applicability.

Imaging techniques utilizing intrinsic optical properties of tissues are free from this drawback. Optical properties of the material are determined by its refractive index, which in general form is a complex, nonlinear function of the frequency and intensity of the incident light. For example, phase contrast microscopy, or optical coherence tomography detect variations of the real linear component of the refractive index within the sample [4]. Some nonlinear imaging methods, such as second- and third-harmonic generation utilize second and third order susceptibility of the material. Imaginary part of the index, responsible for absorption, is also frequently used to identify molecular composition of the tissue. Infrared (IR) microscopy is one of the techniques with chemical contrast based on rich spectral composition of the molecular vibrations corresponding to the IR part of spectrum. However, long wavelengths of mid-IR radiation limit the spatial resolution to several micrometers, and are difficult to use with aqueous samples due to strong water absorption. These issues are circumvented in Raman microscopy, which utilizes visible and near-IR radiation to detect spectral shifts related to specific molecular vibrations. Typically small cross-sections of the non-elastic (Raman) scattering require high power laser sources. It is also often difficult to separate Stokes radiation from the fluorescent background since both types of emission are shifted towards longer wavelengths.

Coherent anti-Stokes Raman scattering (CARS) can greatly enhance the Raman signal utilizing the induced rather than spontaneous emission mechanism. In addition, since the anti-Stokes wavelengths are shorter than the excitation light, CARS signal is free from the fluorescent background. Several applications of CARS to imaging of various biological samples have been recently demonstrated, including intracellular lipid membranes [5], lipid bilayers constituting erythrocyte walls [6], and collagen-rich fascia tissue [7]. CARS also proved to be useful in semiconductor industry – visualizing UV lithographic patterns applied to wafers coated with polymer photoresists [8].

Typically CARS is generated by two tightly co-focused beams (pump and Stokes) that are scanned over the sample, so that the image is created point-by-point using filtered out CARS signal. Due to non-linear nature of CARS, appreciable amount of signal is generated only in a small focal volume (typically less than 1μm in diameter), which allows for high lateral and axial resolution. Though scanning approach is widely adopted nowadays, it has certain shortcomings. High pulse-to-pulse amplitude stability and synchronization of two laser beams are required for artifact-free imaging. Sample scanning is time-consuming and only recently a video-rate regime was demonstrated.

A new method of CARS microscopy – wide-field imaging has emerged a few years ago [9]. This technique potentially allows for simultaneous imaging of much larger field - on the order of thousands μm^2. Two approaches to a wide-field CARS microscopy have been demonstrated so far. The first is based on an illumination geometry, which leads to formation of a thin "sheet of light" [10] within the sample with laser beams satisfying phase matching conditions. Low thickness of the illuminated area helps to maintain relatively low level of the background CARS signal generated in the bulk. Oil droplets and adipocyte liposomes were successfully imaged using this approach in the field of view as large as $1600\mu m^2$ [10].

The second approach is based on illumination of the whole volume of a sample in a non-phasematching geometry, which prevents signal generation in the bulk. This technique relies

#106549 - $15.00 USD Received 21 Jan 2009; revised 5 Mar 2009; accepted 7 Apr 2009; published 20 Apr 2009

on refraction of light on variations of the refractive index within the sample associated with its chemical and mechanical structure. As a result, a fraction of the scattered pump and Stokes beams falls under the phase-matching condition. If the sample contains Raman-active molecules, CARS signal will be efficiently generated in a volume adjacent to the particular scattering center. Chemical selectivity of the method has been demonstrated by imaging a mixture of polystyrene and glass beads of similar diameters using pump and Stokes beams with frequency difference corresponding to aromatic C-H stretch vibration in polystyrene [11].

The latter system initially included a picosecond Ti:Sapphire laser and a frequency doubled optical parametric amplifier (OPA) were used as a pump- and Stokes-beam sources, respectively [11]. OPA, while providing a broad tuning range, has relatively low efficiency (~1%) and significant pulse-to-pulse energy variations (~10%), which limited practical value of this method. Since one of the most common targets in CARS imaging is C-H bonds in lipids, it was deemed reasonable to build a laser system specifically tuned to one of C-H resonances. Such system, while lacking tunability, could be made much more efficient and stable, which would be beneficial for many practical applications.

In the present work we demonstrate a relatively simple implementation of a fixed wavelength CARS system, and further investigate illumination geometries for achieving high spatial resolution and rapid image acquisition.

2. Materials and methods

2.1 Wide-field CARS imaging system

The experimental setup with axially symmetric illumination is shown in Fig. 1. An output beam of a regenerative Ti:Sapphire amplifier (Spectra-Physics, CA) (1ps, 800nm, 1mJ pulses at repetition rate up to 1 kHz) was split by a 30/70 beam splitter. Smaller fraction of the beam (0.3mJ) was further attenuated to prevent damage to optical components and then used as a pump. The other beam was directed into a 0.5m long Raman converter (Light Age Inc., NJ), filled with methane (CH_4) at 2MPa pressure to generate Stokes beam. Methane was an obvious choice since its Raman frequency shift 2914 cm^{-1} is determined by the C-H molecular bond - the most common CARS imaging target in biological samples [12]. Most lipids exhibit several strong resonances within the 2800-3000 cm^{-1} range. In particular, aliphatic C-H stretch vibration located at 2900cm^{-1} has a linewidth of 10cm^{-1}. Transform limited bandwidth of 1ps pulses produced by our laser system also had ~10cm^{-1} linewidth, therefore aliphatic C-H stretch is readily accessible to CARS detection by the aforementioned laser source. Methane-filled Raman converter provided ~10% conversion efficiency producing up to 70 μJ Stokes pulses. Since pump and Stokes pulses were generated by the same laser source they were intrinsically synchronized.

As described earlier [11], the non-phasematching illumination geometry most favorable for efficient CARS generation is comprised of a normal incident pump beam and a converging coaxial annular Stokes beam. In our experiment pump beam collimated with a long focal length lens (f = 1m) was directed normal to the sample plane, producing ~500 μm diameter Gaussian spot. Only a central part of the spot (~170μm diameter) was used to assure that non-uniformity of the light intensity does not exceed 20%.

#106549 - $15.00 USD Received 21 Jan 2009; revised 5 Mar 2009; accepted 7 Apr 2009; published 20 Apr 2009

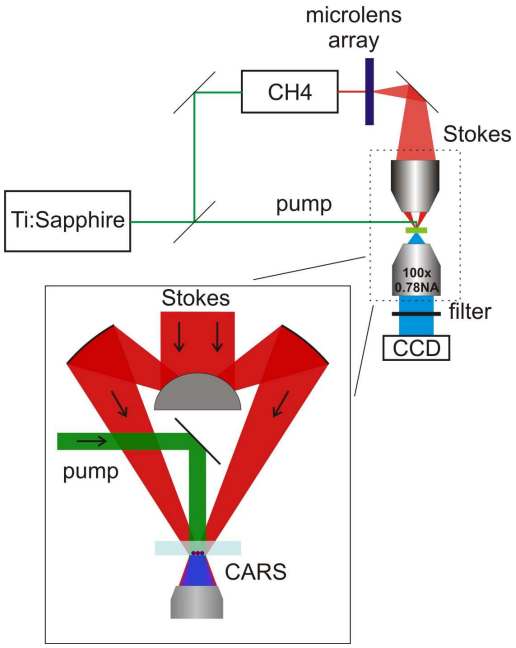

Fig. 1. Diagram of the experimental setup, with a closeup showing orientation of the pump, Stokes and CARS beams, relative to the sample and imaging objective. Cassegrain objective is represented by its internal mirrors.

Stokes beam was focused with a Cassegrain objective (NA = 0.28), providing a range of angles 9° – 16° with respect to the pump beam. To produce a 200μm diameter spot at the focal plane, an irregular divergence has been introduced to the beam by a microlens array. Application of such homogenizer to a coherent beam inevitably produces interference pattern in the object plane. To quantify the homogeneity of the Stokes beam we acquired two-photon fluorescence pattern in a thin (~10μm) layer of methanol solution of Rhodamin B (see Fig. 2(a)). Taking into account that fluorescent signal depends quadratically on the excitation light intensity, we derived from this imaging data that the intensity in the Stokes beam varies by a factor of 5 over the illuminated spot. To average this interference pattern out, the microlens array was irregularly translated perpendicularly to the laser beam from shot to shot by ~100 μm. About 100 pulses were required to reduce variability in illumination to 10% level (Fig. 2(b)). Average fluences over the 200μm illuminated area for pump and Stokes beams were 100mJ/cm^2 and 18mJ/cm^2, respectively.

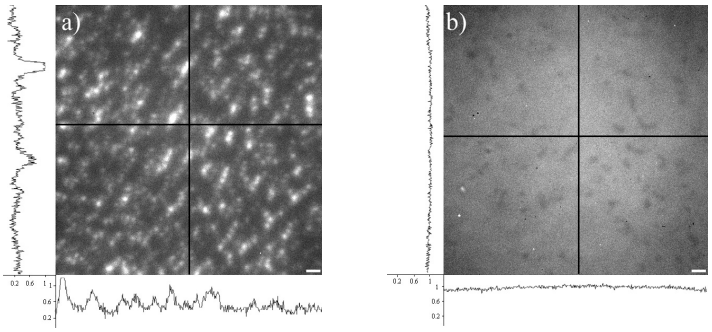

Fig. 2. (a). Two-photon fluorescence images produced by Stokes beam in a 10μm layer of Rhodamin B solution; (b) Stokes beam averaged out by irregular movement of microlens array (scale bar is 10μm). Intensity profiles along the black lines are indicated to the left and at the bottom of each image.

#106549 - $15.00 USD Received 21 Jan 2009; revised 5 Mar 2009; accepted 7 Apr 2009; published 20 Apr 2009

Averaging of the interference pattern caused by the microlens array limits the image acquisition speed in this approach to approximately 100 pulses. To allow for a single pulse image acquisition we applied another illumination scheme, producing relatively homogenous beam distribution over an extended area without interference (Fig. 3). In this approach both pump and Stokes beams are collimated by long focal length lenses (f = 1m) and directed onto the sample in a common plane of incidence at 70° and 60° with respect to the microscope objective axis. Similar to the first setup, only central part of beams was used to achieve ~20% uniformity of illumination within ~200μm diameter field. Mechanical shutters were introduced in paths of both beams to ensure that only one pair of pulses is delivered to the sample. Since the excitation beams were directed outside the collection angle of the microscope objective, higher intensities could be applied without endangering the microscope optics. In this approach we applied pump and Stokes pulses with fluences of 750mJ/cm^2 and 100mJ/cm^2, respectively. These values are comparable to total fluence used for a single frame acquisition in typical scanning CARS systems [13].

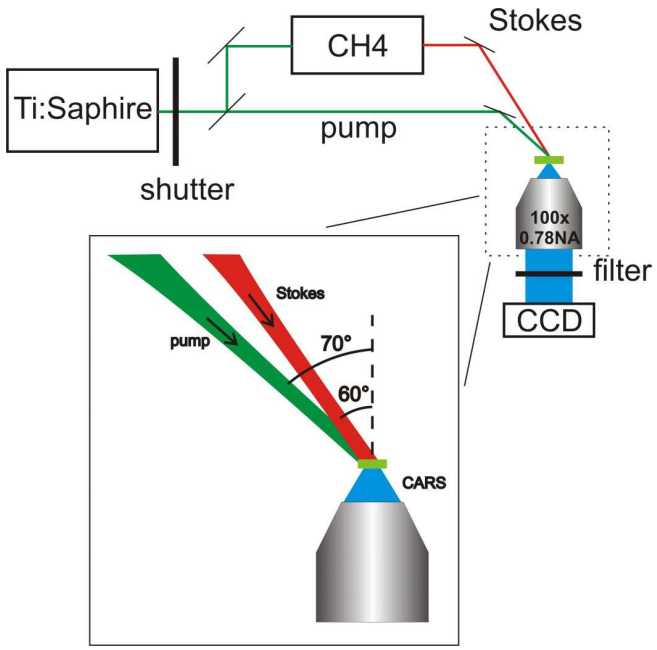

Fig. 3. Experimental system for single-shot CARS imaging. Closeup shows pump and Stokes direction with respect to the axis of microscope objective.

CARS signal at 650nm was detected in forward direction (i.e. F-CARS). Samples were imaged using 100x objective (NA = 0.78) and images were captured by a liquid nitrogen cooled CCD camera (CCD-512-TKB/1/VISAR, Princeton Instruments). A set of filters was installed in front of the camera to suppress pump and Stokes radiation by ~6 orders of magnitude, while retaining ~80% transmission at CARS wavelength. For more precise evaluation of contrast between resonant signal and non-resonant background the dark frames of the camera (images with the camera shutter closed) were subtracted from the CARS images.

2.2 Sample preparation

Polystyrene beads of 1 and 3μm in diameter, as well as rat spinal cord tissue sections were used as sample targets. The beads were deposited on 10μm thick Mylar film or on 120μm thick glass coverslip (micro cover glass No. 1, VWR). The film was either kept dry, or was

#106549 - $15.00 USD Received 21 Jan 2009; revised 5 Mar 2009; accepted 7 Apr 2009; published 20 Apr 2009

covered with a 1mm layer of water. Spinal cord tissue contains lipid-rich myelin sheath (~70% of lipids by weight), and the large number of C-H bonds in lipids act as an excellent marker for CARS imaging [14].

Cryo-sections of spinal cord tissue from euthanized RCS rat, embedded in Optimal Cutting Temperature (OCT) medium were cut using a cryomicrotome (2800 Frigocut N, Reichert). To avoid multiple scattering in the tissue, sufficiently thin (~6μm) sections were used. The longitudinal and cross sections of spinal cord were picked up on glass microscope slides, immersed in phosphate buffered saline (PBS) and sandwiched between a 120μm coverslip and 10μm Mylar film, with the film facing the microscope objective.

For comparison, some sections were stained with FluoroMyelin green fluorescent dye (Invitrogen, Ltd., UK) that specifically stains myelin. All the sections were briefly rinsed in PBS, coverslipped and photographed.

In addition, histological sections of the same tissue were prepared and imaged using a visible light microscope. The samples were fixed in a mixture of gluteraldehyde and paraformaldehyde, embedded into the epoxy medium, sectioned and stained with toluidine blue.

3. Results and discussion

3.1 Spatial resolution

Image of 1 μm polystyrene beads on Mylar film in air, acquired with 100 pulses, is shown in Fig. 4(a). CARS nature of the signal was verified by varying a delay between the pump and Stokes pulses. Magnified views in insets demonstrate that the neighboring beads are clearly resolved. The ratio of the bead brightness to the background level after a dark frame subtraction was 10:1. Spatial resolution in our CARS system is determined by the imaging objective. For NA = 0.78 and signal wavelength λ_{CARS} = 650nm the diffraction limited resolution is 0.5μm. We derive similar value when applying Rayleigh resolution criterion to the beads emission intensity profiles shown in the lower inset in Fig. 4(a).

Biological samples are often imaged in physiological medium, with refractive index practically equal to that of water. To characterize the effect of higher refractive index medium on image quality we acquired similar images of 1μm beads in water, as shown in Fig. 4(b). Contrast of the beads in this image reduced to 6:1. However, they are still clearly visible and resolvable over the whole field of view.

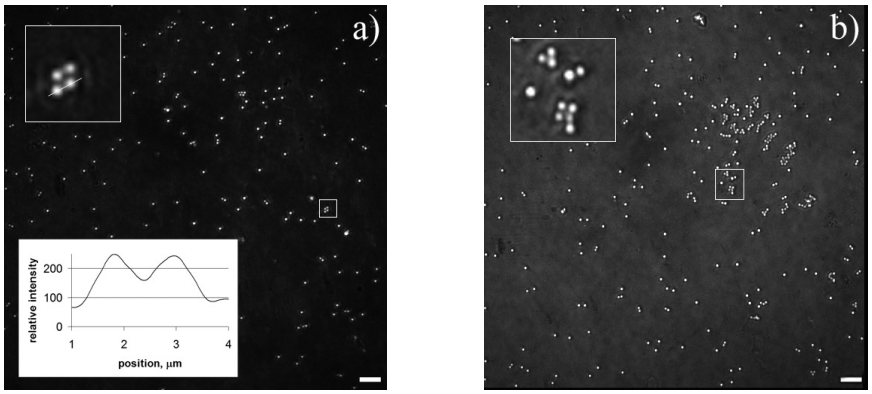

Fig. 4. (a). CARS image of 1μm polystyrene beads on a 10 μm Mylar film in air; bottom insert shows relative intensity profile along the white line; (b) CARS image of 1μm beads on a Mylar film immersed in water (scale bar is 10μm).

#106549 - $15.00 USD Received 21 Jan 2009; revised 5 Mar 2009; accepted 7 Apr 2009; published 20 Apr 2009

3.2 Myelin specific image contrast in the nerve tissue

CARS images of longitudinal and transversal sections of rat spinal cord are shown on Figs. 5(a) and 5(b), respectively. Lipid-rich myelin sheath forming nerve boundaries is clearly seen against the dark non-resonant material (with low lipid content), with contrast 5:1. The level of signal from the non-myelinated part of tissue is comparable to the background signal from saline solution and glass cover slip.

To confirm that bright pattern observed in CARS images of the unstained samples corresponds to myelin sheaths we compared them to bright-field and fluorescent images of the stained samples. Spinal cord sections stained with myelin-specific fluorescent dye, and histological samples stained with toluidine blue are shown in Figs. 5(c)-5(f). It is clearly seen that bright structures in CARS images correspond well to regions containing myelin sheaths in spinal cord tissue.

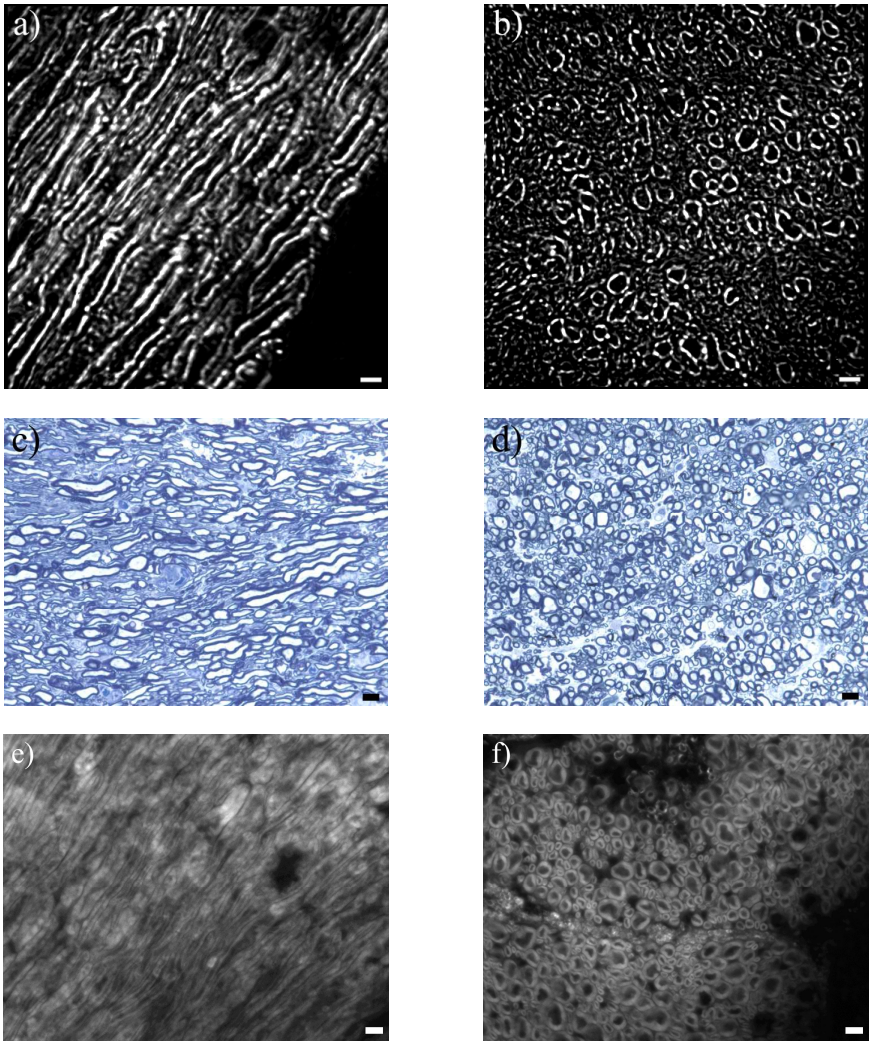

Fig. 5. (a)-(b) CARS images of the longitudinal and cross-sections of the rat spinal cord, respectively; (c)-(d) images of histological samples of the same tissue stained with toluidine blue; (e)-(f) fluorescent images of the same tissue stained with myelin-specific dye (FluoroMyelin green). Scale bar is 10μm in all images.

#106549 - $15.00 USD Received 21 Jan 2009; revised 5 Mar 2009; accepted 7 Apr 2009; published 20 Apr 2009

These images demonstrate selective contrast of the described system to lipid-rich tissue structures, and its applicability to imaging of tissue layers and cell cultures without exogenous staining.

The system operates with pulse fluence of 100mJ/cm^2 per pulse, and total fluence (integrated over 100 pulses) of 10J/cm^2. For comparison, in scanning system operating at 76 MHz with average power of 50 mW and spot size of 0.3 μm, the pulse fluence is 0.2 J/cm^2. With a frame size of 0.5 mm^2, and frame acquisition time of 30 ms the total fluence per frame is 0.3 J/cm^2.

3.3 Single-pulse imaging

Images of 3μm polystyrene beads in air acquired with a single pair of pulses, shown in Fig. 6(a), demonstrate a possibility of visualizing a 200 μm area within a single exposure of 1ps in duration. Frame rate in such imaging is limited by the laser repetition rate and the camera readout time. CARS nature of the signal was verified by varying a delay between the pump and Stokes pulses. No difference was detected between the images of beads placed on 10 μm Mylar film and those placed on 120 μm glass coverslip. The absolute brightness of beads was the same in both cases, indicating that CARS signal was generated in the polystyrene beads rather than in an underlying substrate. The ratio of bead brightness to the camera dark noise was approximately 10:1. However, it was not possible to accurately evaluate the image contrast since the amount of the background CARS signal was below the detection limit. When imaging 1μm beads the signal level was comparable to noise, setting a limit to sensitivity of the single pulse imaging.

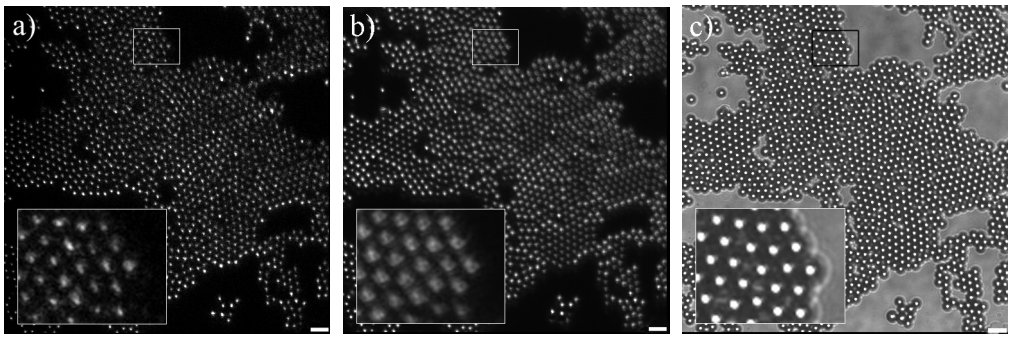

Fig. 6. (a). CARS image of 3μm polystyrene beads obtained with a single pair of pulses; (b) bright-field image of the same sample of 3μm beads with non-symmetrical illumination; (c) bright-field image of the same sample with correct illumination. The insets show single bead profile along two perpendicular directions (scale bar is 10μm).

Since the pump and Stokes beams illuminate the sample from only one side, CARS signal is not emitted isotropically either, which reduces the resolution and degrades image quality. As a result, the images of the 3 μm beads have a distorted (asymmetric) shape. Illumination with collimated beams known to be unfavorable for microscopy, also contributes to this distortion effect. Similar distortions can be observed with asymmetric white light illumination. For example, Fig. 6(b) shows an image acquired with white light directed at ~70° with respect to the microscope objective axis. Using axially symmetric illumination restores the image quality, as expected (Fig. 6(c)).

One of the major advantages of single-shot CARS imaging is its inherently short exposure time required for frame acquisition. In the example shown above, the frame was acquired in 1ps, which is more than 10 orders of magnitude shorter than corresponding time in scanning technique. Such a short acquisition time might be useful to capture short-living states, rapid transitions or fast moving objects in a number of applications.

#106549 - $15.00 USD Received 21 Jan 2009; revised 5 Mar 2009; accepted 7 Apr 2009; published 20 Apr 2009

4. Conclusions

We described a wide-field CARS microscopy system with methane-filled Raman converter for generation of Stokes beam, which simplifies the setup, ensures appropriate frequency difference for C-H aliphatic stretch, and provides inherent synchronization between pump and Stokes photons. The spatial resolution of the system with proper illumination was shown to be close to diffraction limit of the imaging objective. We demonstrated selective contrast to lipid-rich myelin sheaths in imaging of the nerve tissue.

We have also demonstrated, for the first time, a wide-field CARS system capable of acquiring images with a single pair of pulses of 1ps in duration. For this system, further development of proper axially symmetric illumination with homogenous pump and Stokes beams will allow for full utilization of the advantages of the wide-field CARS imaging in non-phase matching illumination geometry.

Acknowledgments

Authors would like to thank Philip Huie for providing nerve tissue samples. This work was supported by the Air Force Office of Scientific Research (MFEL grant).

#106549 - $15.00 USD Received 21 Jan 2009; revised 5 Mar 2009; accepted 7 Apr 2009; published 20 Apr 2009